Development of A Maximum Anti-Slosh Baffle Pressure Load Model

H. Q. Yang
NASA Marshall Space Flight Center, Alabama, USA

M. D. Sansone
NASA Marshall Space Flight Center, Alabama, USA

J. M. Brodnick
NASA Marshall Space Flight Center, Alabama, USA

Brandon Williams
NASA Marshall Space Flight Center, Alabama, USA

ABSTRACT

The sloshing of propellants can affect the stability of a spacecraft and the integrity of the tank structure. Undesirable sloshing can be controlled by the addition of anti-slosh baffles, and the spacing and configuration of baffles are driven by damping requirements. The structural design of the baffle is determined after consideration of many factors, such as the strength and rigidity needed to support the baffle for its lifetime. Therefore, knowledge of distributed pressure loading is important for detailed structural design. In addition, the resultant force and moment produced by the distributed pressure are of direct importance to the design of a vehicle's control system. Previous experimental investigations have been conducted to determine the liquid pressure loads and slosh damping associated with a rigid ring baffle. The results suggested that when the nondimensional velocity parameter is larger than 1.0, the theories agree with the test. However, when the velocity parameter is less than 1.0, all theories are non-conservative and under-predict the pressure loads. The present study has derived a maximum pressure load on the slosh baffle based on the energy conservation principle. It is verified from CFD that pressure in the slosh flow field can be decomposed into static and transient components. The CFD results confirm that there is a phase shift in pressure across the baffle, which depends on the fluid damping. Higher damping leads to a higher phase shift. The CFD investigation further verifies the proposed theory: the maximum pressure load occurs when the phase shift is 90 degrees. A comparison of the present computational results to the previous comprehensive experimental data validates the maximum pressure theory. When the baffle is submerged, the maximum pressure theory envelopes all the experimental data points.

INTRODUCTION

Propellant slosh is a potential source of disturbance critical to the stability of space vehicles. The slosh dynamics are typically represented by a mechanical model of a spring-mass damper. This mechanical model is then included in the equations of motion for the entire vehicle used in Guidance, Navigation, and Control analysis. The typical parameters required by the mechanical model include the

slosh mode natural frequency, slosh mass, slosh mass center location, and the critical damping ratio. During the 1960s U.S. space program, these parameters were either computed from an analytical solution for a simple geometry or by experimental testing for the sub-scale configuration. Previous work by the authors [1] has demonstrated the soundness of a CFD approach in modeling the detailed fluid dynamics of tank slosh and has shown excellent accuracy in extracting the mechanical properties for different tank configurations and at various fill levels. The validation studies included comparisons of CFD solutions for a straight cylinder against an analytical solution and for sub-scale Centaur liquid oxygen (LOX) and liquid hydrogen (LH2) tanks with and without baffles against experimental results for the natural frequency, slosh mass, and slosh mass center location. The study showed that CFD methods could provide accurate mechanical parameters for any tank configuration and is especially valuable for the future design of propellant tanks, as experimental data is not available for every propellant tank configuration.

Since the liquid oscillatory frequency may nearly coincide with either the fundamental elastic body bending frequency or the dynamic control frequency of the vehicle at some time during the powered flight, slosh forces can interact with the structure or control system. This can cause a failure of structural components within the vehicle or excessive deviation from its planned flight path [2]. Therefore, it is necessary to consider means of providing adequate damping of the liquid motion and slosh forces and to develop methods for accounting for such damping in the vehicle performance analyses.

To meet the damping requirement for a flight controller, baffles of various configurations have been devised to augment the natural viscous damping of slosh waves and decrease the magnitude of slosh forces and torques [2]. However, there exists a strong desire to minimize launch vehicle weight, including the use of lightweight propellant tanks with minimal to no baffles. One of the challenges in reducing the baffle weight is the structural stress acting on the baffle. The structural design of the baffle is determined after considering many factors, such as the strength and rigidity needed to support the baffle for its lifetime. Therefore, the distributed pressure loading on the baffle is important for detailed structural design. In addition, the resultant force and moment produced by the distributed pressure are of direct importance to the design of a vehicle's control system.

A previous study by Liu demonstrated an analytical technique for determining the pressure force on a ring baffle due to irrotational sloshing [4]. Davis derived a semi-theoretical expression for pressure, which includes both fluid acceleration and liquid velocity [5]. In the NASA monograph "Propellant Slosh Loads" [6], the maximum pressure acting on a submerged baffle subject to the oscillatory velocity of sloshing liquid is expressed as a parameter determined by Keulegan and Carpenter's experiment [7].

A comprehensive experimental investigation was conducted by Scholl *et al.* [5] to determine the liquid pressure loads and slosh damping associated with the rigid ring baffle. The report [5] contains the complete set of publicly available baffle pressure test data. It covers a range of depths and values of period parameters. Some of the results are shown in Figure 1. One can see that at nondimensional velocity parameters larger than 3.0, all theories seem to predict the pressure well. However, for lower velocity parameters between 0.5 and 3.0, the theories under-predict the pressure load (see Figure 1). These results suggest that when the baffle is submerged, the theories agree with the test. However, when the baffle is exposed, all theories are non-conservative and under-predict the pressure loads.

The purpose of this paper is to develop a fundamentally sound maximum pressure load model that matches the experimental data across the range of baffle depths and wave heights. This will be accomplished by deriving a theory of the maximum possible pressure on a baffle. As shown later in the derivation, the maximum pressure derived from the present theory is found to be $\sqrt{2}\rho g\eta$, with η as the slosh wave height.

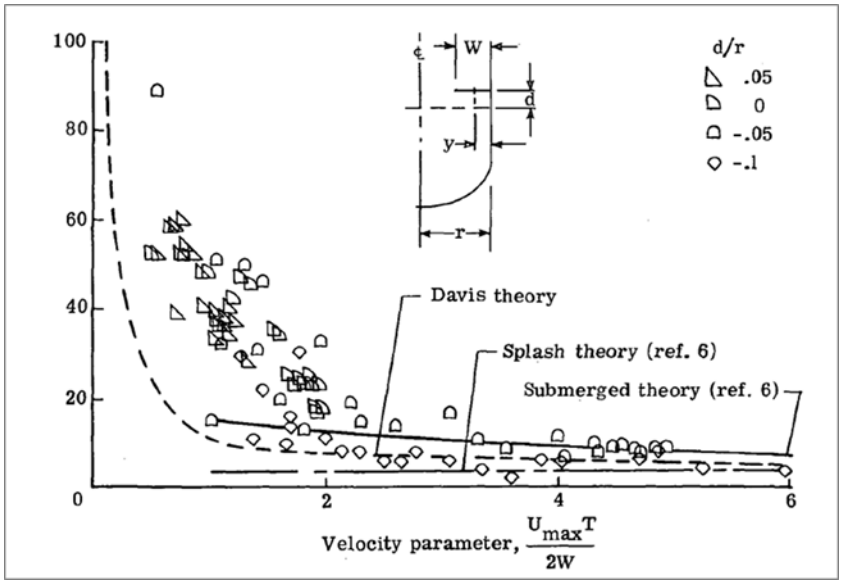

Figure 1. Previous development of the theoretical model on nondimensional pressure with nondimensional velocity parameter [5]

Development of Analytical Solution

Slosh Pressure Load Theory

The following describes the derivation of the proposed maximum slosh pressure load theory. The basis of this theory will subsequently be verified using high-fidelity CFD simulations.

It is known that slosh dynamics can be described using spring-mass-damper models. During one slosh period, slosh represents a dynamic transfer process between potential energy and kinetic energy. The potential energy is $\rho g \eta$, and the kinetic energy is formed from the mass of the slosh mass and its velocity. See Figure 2 for the definition of wave height η.

Based on Bernoulli's principle:

$$\frac{v^2}{2} + \rho g \eta + p = constant \tag{1}$$

The maximum oscillatory pressure amplitude (which occurs when the wave reaches the peak and velocity is zero) is:

$$p_\eta = \rho g \eta \tag{2}$$

One can write the pressure at a given point in the tank as the summation of static pressure (when there is no slosh) and transient pressure (due to slosh):

$$p = p_{static} + p_{transient} \tag{3}$$

Since bulk slosh motion can be described by a sinusoidal function, the transient pressure is:

$$p_{transient} = p_\eta \sin(\omega t + \theta); \text{ with: } \max(p_\eta) = \rho g \eta \tag{4}$$

Neglecting the difference in static pressure across the baffle, the dynamic pressure differential across the baffle from Equation (4) is:

$$\Delta p = p_\eta \, sin(\omega t + \theta_1) - p_\eta \, sin(\omega t + \theta_2) = p_\eta [sin(\omega t + \theta_1) - sin(\omega t + \theta_2)] \quad (5)$$

where θ_1 is the phase angle at the top of the baffle relative to the free surface wave. θ_2 is the phase angle at the bottom of the baffle relative to the free surface wave. The phase shift between the top and bottom of the baffle ($\theta_1 - \theta_2$) is due to damping in the fluid. The maximum of Eq. (5) occurs at a phase shift of 90 deg, where we obtain the highest pressure load of:

$$\Delta p_\eta = \max \left(p_\eta [\sin(\omega t + \theta_1) - \sin(\omega t + \theta_2)] = \sqrt{2} \rho g \eta \right) \quad (6)$$

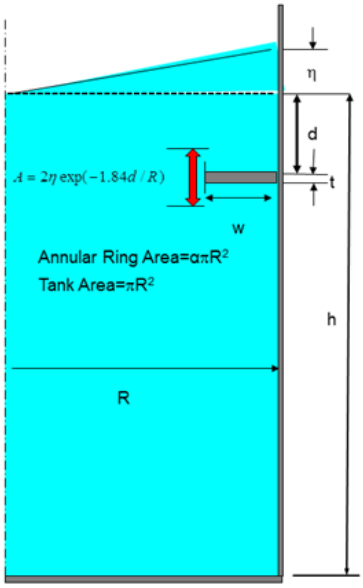

Figure 2. Definition of related quantities for a submerged baffle. h: liquid fill level; η: wave height; d: baffle depth from the free surface; R: liquid tank radius; w: baffle width.

CFD Verification of Slosh Pressure Load Theory

A CFD model has been built to verify the proposed pressure load theory. The model is shown in Figure 3, and it has the following parameters:

- Cylindrical tank with tank radius, R = 165";
- The liquid fill level from tank bottom, h = 2R; baffle width (W): 12";
- Liquid: LH2; density: 70.8 kg/m^3;
- Initial wave height: η = 4";
- Baffle depth, d: d/R = 0.0, 0.05, 0.1, 0.25;
- Total number of cells: 0.5 million;
- Pressure monitor points from tank wall: 0.25W, 0.5W, 0.75W.

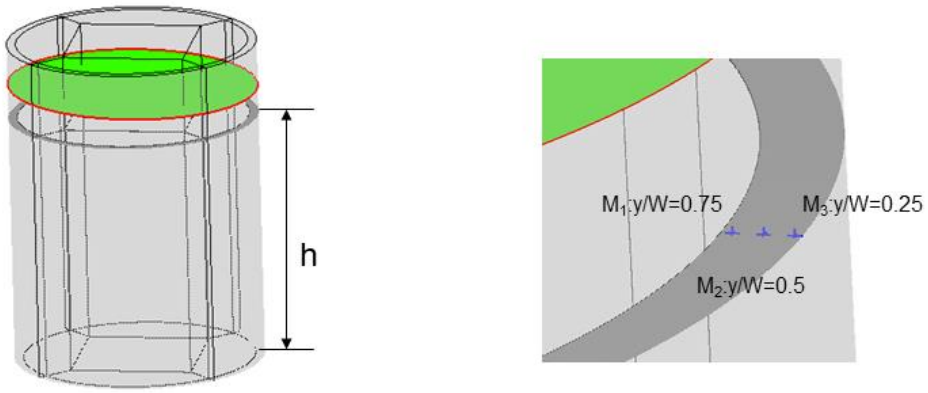

Figure 3. CFD model used to verify the maximum pressure load theory. The red line is the fluid and gas interface, and the baffle is submerged.

Verification #1: Max Local Transient Pressure Magnitude is $\rho g \eta$

We propose pressure can be decomposed into static and transient components.

$$p = p_{static} + p_{transient} \tag{7}$$

$$p_{transient} = p_{\eta} \sin(\omega t + \theta);\ \text{with:}\ \max(p_{\eta}) = \rho g \eta \tag{8}$$

The maximum transient amplitude is $\rho g \eta$, and η is the initial wave height. Figure 4 shows the CFD results for mid-width (0.5W) transient pressure at a point above the baffle, a point below the baffle, and the transient pressure difference between the two at three baffle depth ratios (d/R=0.25, d/R=0.1 and d/R=0.0). The transient pressure is referenced to the local static pressure and is normalized by the predicted max transient pressure (shown in Equation (8)) with an initial wave height of 4" ($\rho g \eta$).

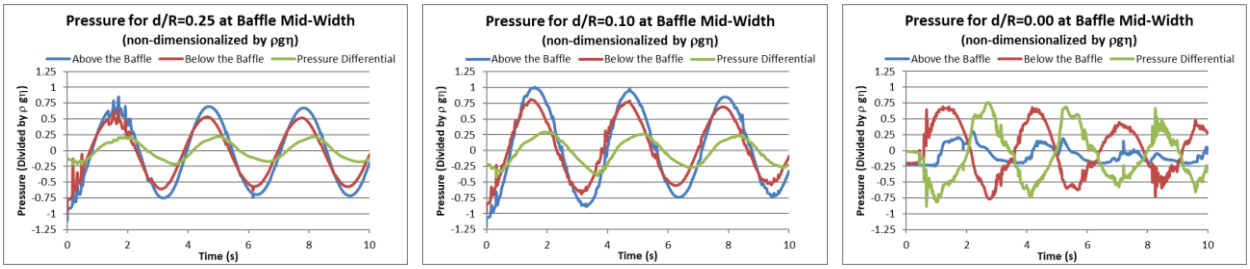

Figure 4. Nondimensional transient pressure around baffles at different depth ratios (d/R) from the free surface at the mid-width location

We can see that the pressure inside the flow field is indeed periodic and is at the same frequency as slosh frequency, which is $f = \frac{1}{2\pi}\sqrt{\frac{1.84g}{R}}$=0.330 Hz [2].

Just as proposed, the pressure has static and transient components. The static pressure is nothing but hydrodynamic static pressure $\rho g h$, with h as the distance from the free surface. This static pressure component has been subtracted from the plots in Figure 4. As the transient components contribute to the slosh pressure, they are shown in Figure 4. One can see that the amplitude of the transient component is less than $\rho g \eta$ (1.0 in the figures), with η as the slosh wave height. This verifies that the maximum local transient pressure magnitude is ρgη.

Verification #2: There is a Phase Shift in Pressure Across the Baffle

We propose that the pressure load is:

$$p_{top} = p_\eta \sin(\omega t + \theta_1) \tag{9}$$

$$p_{bottom} = p_\eta \sin(\omega t + \theta_2) \tag{10}$$

One can see from Figure 4 that there is indeed a phase shift in pressure across the baffle which increases as the fill level decreases. For d/R=0.25, $(\theta_1 - \theta_2) = 6.95\ deg.$; for d/R=0.10, $(\theta_1 - \theta_2) = 8.76\ deg.$; and for d/R=0.0, $(\theta_1 - \theta_2) = 88.4\ deg.$ The phase shift is a result of damping inside the fluid. A larger phase shift implies a higher damping. The largest phase shift occurs at d/R=0.0 and is close to 90 deg.

Verification #3: Max Pressure Load is $\sqrt{2}\rho g\eta$

We assume that the pressure phase differs across the baffle.

$$\Delta p = p_\eta[sin(\omega t + \theta_1) - sin(\omega t + \theta_2)] \tag{11}$$

Let us assume that the phase shift has a maximum value of $(\theta_1 - \theta_2) = 90\ deg.$

Use the following expression:

$$\begin{aligned}\Delta p = p_\eta[sin(\omega t + \theta_1) - \sin(\omega t + \theta_1 + 90^o)] &= 2p_\eta sin(\omega t + \theta_1 - 45^0)\cos(45^o) \\ &= \sqrt{2}p_\eta sin(\omega t + \theta_1 - 45^o) = \sqrt{2}\rho g\eta sin(\omega t + \theta_1 - 45^o)\end{aligned} \tag{12}$$

This arrives at our maximum load of $\sqrt{2}\rho g\eta$. Figure 4 includes the pressure differential across the baffle non-dimensionalized by the maximum transient pressure $\rho g\eta$. Based on the above derivation, the maximum pressure across the baffle should be less than $\sqrt{2}$. Figure 4 shows that for both baffle depths of d/R=0.25 and d/R=0.10, the nondimensional values are around 0.25. For the depth ratio of d/R=0.0, the nondimensional value is larger at about 0.75. But the maximum is less than our derivation of 1.41.

Figure 5 shows the transient pressures at the baffle. The results again verify that none of the computed pressure loads across the baffle are higher than $\sqrt{2}\rho g\eta$ ($\sqrt{2}$ in the nondimensional form) at different fill levels.

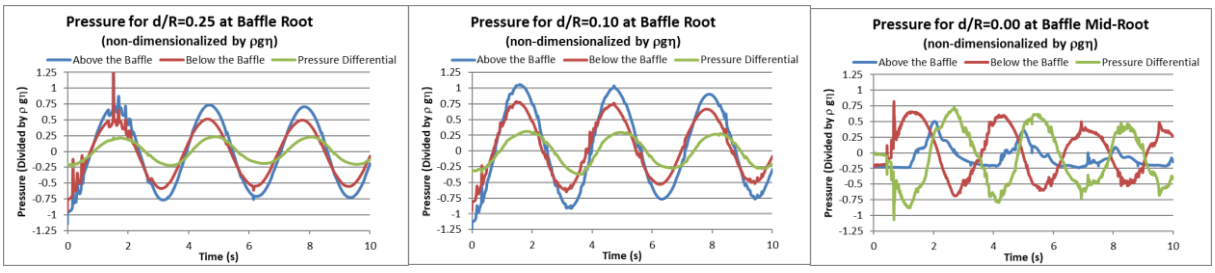

Figure 5. Nondimensional transient pressure load on baffle root at different depth ratios (d/R) from the free surface.

Validation of Slosh Pressure Load Theory

An investigation was conducted by Scholl *et al.* [5] to determine the pressure loads and damping associated with rigid ring baffles in relatively large cylindrical tanks (see Figure 6). The radial and

circumferential pressure distribution, as well as the damping, was measured on a ring baffle subjected to fundamental antisymmetric slosh in a 284cm-diameter rigid tank. Experimental and analytical data are presented as a function of slosh velocity or amplitude, baffle spacing, and baffle locations both above and below the liquid surface.

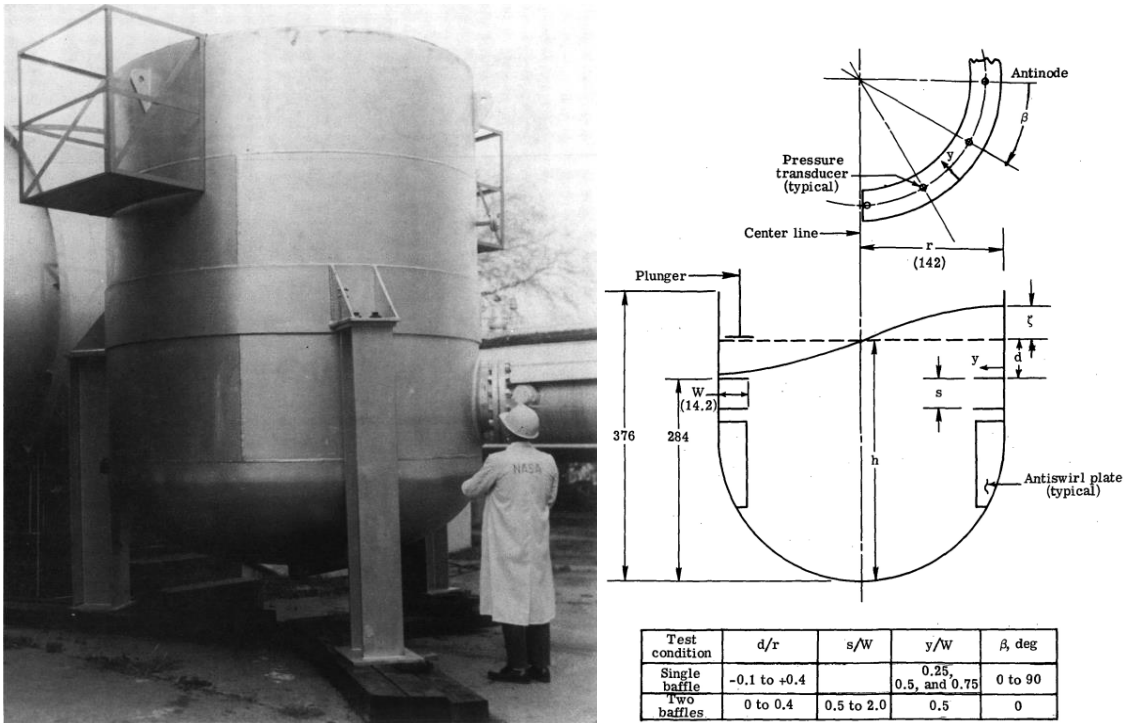

Test condition	d/r	s/W	y/W	β, deg
Single baffle	-0.1 to +0.4		0.25, 0.5, and 0.75	0 to 90
Two baffles	0 to 0.4	0.5 to 2.0	0.5	0

Figure 6. Slosh tank with 284cm diameter (left); tank and baffle variables [5].

The measured pressure data are presented in terms of a reduced velocity parameter $\frac{U_{max}T}{2W}$, which is a nondimensional parameter (often referred to as the period parameter) describing the relative velocity. Here U_{max} is the maximum liquid velocity at the baffle location; T is the natural period of the oscillation, and W is the baffle width. The maximum vertical velocity in a cylindrical tank at the baffle location due to the antisymmetric mode may be written as [5]:

$$U_{max} = \omega\eta_{max} sinh\left(1.84\frac{h-d}{R}\right)/sinh\left(1.84\frac{h}{R}\right) \tag{13}$$

where ω is the natural slosh frequency, η_{max} is the maximum displacement amplitude of the surface, d is the distance of the baffle below the quiescent surface, R is the tank radius, and h is the liquid depth. When the baffle is located at or below the quiescent surface, the value obtained from Eq. (13) at the baffle depth may be used to obtain the value of the reduced velocity parameter.

In the presentation of experimental work and previous analytical results [5], the pressure is non-dimensionalized as:

$$\bar{p} = \frac{P}{\frac{1}{2}\rho {U_{max}}^2} A \tag{14}$$

Let us define: $U_{max} = \omega\eta$, where $\omega = 2\pi f;\ f$: slosh frequency, T: slosh period, and $T = \frac{1}{f}$. Combining with the predicted maximum pressure load from Eq. (6), we have:

$$\frac{p_{max}}{\frac{1}{2}\rho {U_{max}}^2} = \frac{1.41\rho g\eta}{\frac{1}{2}\rho(\omega\eta)^2} = \frac{2.82g}{\omega^2\eta} \tag{15}$$

For a straight cylinder with a neglected bottom effect, one has [2]:

$$\omega^2 = \frac{1.84g}{r}, \qquad \text{and} \quad \frac{U_{max}T}{2W} = \frac{\pi\eta}{W} \tag{16}$$

Now, our nondimensional maximum pressure load will be:

$$\overline{p_{max}} = \frac{p_{max}}{\frac{1}{2}\rho {U_{max}}^2} = \frac{4.81}{\left(\frac{U_{max}T}{2W}\right)}\left(\frac{R}{W}\right) \tag{17}$$

It should be emphasized that the nondimensional baffle pressure load is not only a function of the nondimensional velocity parameter but also a function of the baffle width-to-tank radius ratio.

Shown in Figure 7 are the experimental data (black symbols), the previous theories (black lines), the current CFD simulation (red symbols), and our maximum pressure theory (blue line) at the baffle quarter width location of $y/W = 0.25$. The results for different baffle depths are plotted together. First, we notice that Davis' theory matches with experimental data very well when the velocity parameter is larger than 1. For the lower velocity parameters of less than 1.0, however, the theory under-predicts the pressure. The current CFD results are consistent with the experiment of Scholl *et al.* [5] in that the data fall within the experimental data range, which validates the accuracy of those predictions. The present maximum pressure theory generally envelopes the data, except for a few experimental points where the baffle is at or above the free surface.

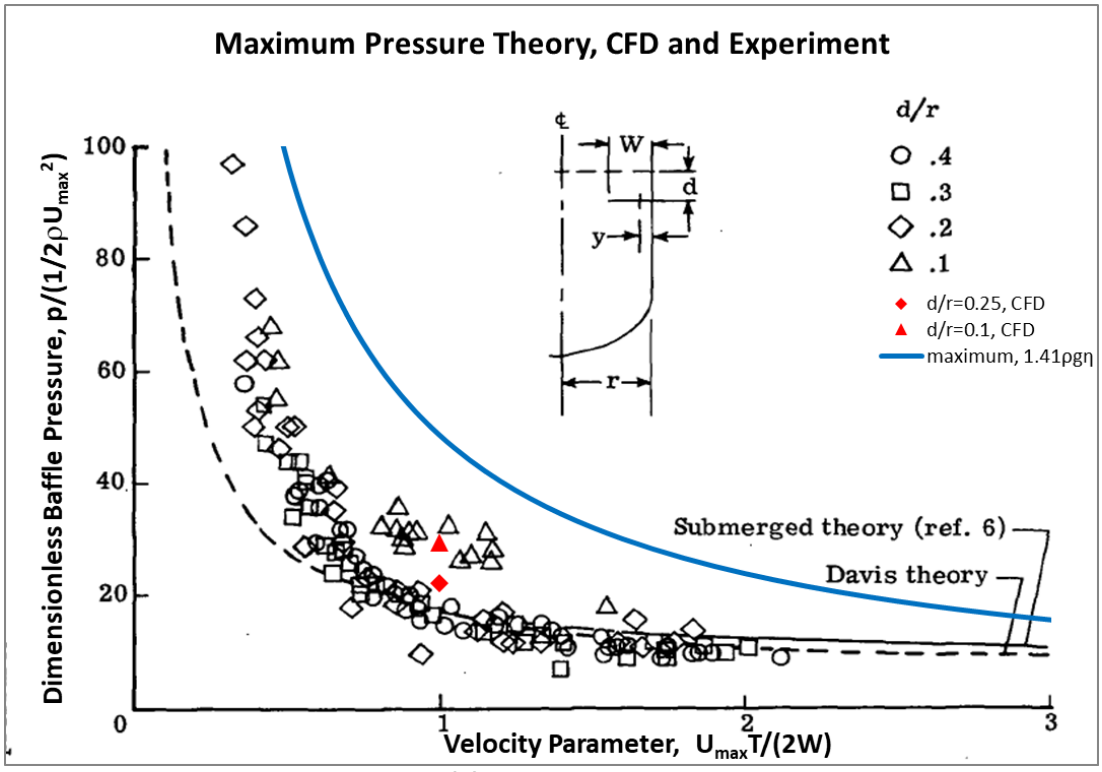

(a) Submerged baffle

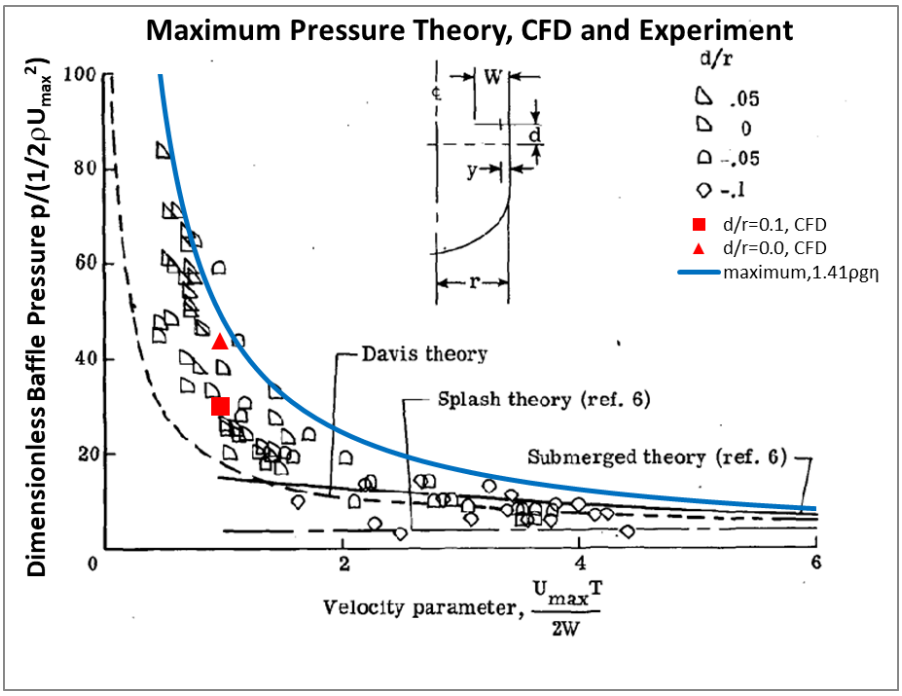

(b) Baffle near the free surface

Figure 7. Pressure comparison at baffle quarter width ($y/W = 0.25$) between experimental data, previous theories, CFD, and the current maximum pressure theory

Shown in Figure 8 are the experimental data (black symbols), the previous theories (black lines), the current CFD simulation (red symbols), and our maximum pressure theory (blue line) at the middle of the baffle ($y/W = 0.50$). The results for different baffle depths are plotted together. Again, we notice that Davis' theory matches with experimental data reasonably well when the velocity parameter is larger than 1. However, the discrepancy between the theory and the experimental data is rather large for the lower velocity parameters of less than 1.0. The CFD simulation predictions fall within the experimental data range [5]. One can clearly see that our maximum pressure theory greatly improves the predictive capability of Davis' theory and envelopes all the submerged baffle depth positions. From Figure 8, we notice that for some data points of $d/R < 0$, which is the case when the settled free surface is lower than the baffle surface, there are pressure values from the experiment which exceed the maximum pressure theory predictions. To investigate the feature of the high-pressure values, we conducted extra simulations at d/R=-0.05, with an initial wave height of $\frac{\eta}{R} = 0.1$. The local transient pressure values at several points on the baffle are shown in Figure 9.

Indeed, when the liquid fill level is close to the baffle, or when d/R is small, if the wave height is larger than the baffle depth ($\eta/R > d/R$), the liquid will splash the baffle. In addition to an increase in slosh damping, the impact of liquid on the baffle produces a high-pressure pulse with an amplitude higher than that of the proposed maximum pressure. CFD simulation results demonstrate these dynamics and reveal that the high collision pressure is localized and has a time scale much smaller than the slosh period. Splash loads and slosh loads should be separated as distinct phenomena for load analyses due to how differently they transfer energy to the baffle structure.

Slosh loads periodically excite baffles at a low frequency distributing energy into low-order structural modes, which typically also have lower inherent damping, thus allowing excitation to persist for relatively longer. Splash loads excite higher-order structural modes, which commonly have higher damping, but the loading is also applied either impulsively or at a much lower slosh frequency. As such, splashing cannot

excite a higher-order baffle mode at resonance, which would yield unbounded amplitude growth. Consequently, splash loads may not present as many challenges to baffle designers as slosh loads.

Additionally, Figure 9 shows the slosh loads during splashing are still bounded by the proposed maximum pressure theory demonstrating the validity of the model even at fill levels very near the baffle location. Given the nature of slosh dynamics when the free surface directly interacts with the baffle, it is believed that the experimental data at fill levels very near the baffle location contains both slosh and splash loads. The pedigree of the data and data analysis is not fully known, so it is impossible to verify if the reported pressures do contain splash loads.

Figure 10 shows the comparison of the present theory with experimental data at the tip of the baffle ($y/W = 0.75$). Again, we see that the predicted pressure load from CFD is in good agreement with the experimental measurement, and the proposed maximum pressure theory load of $1.41\rho g\eta$ conservatively bounds the data.

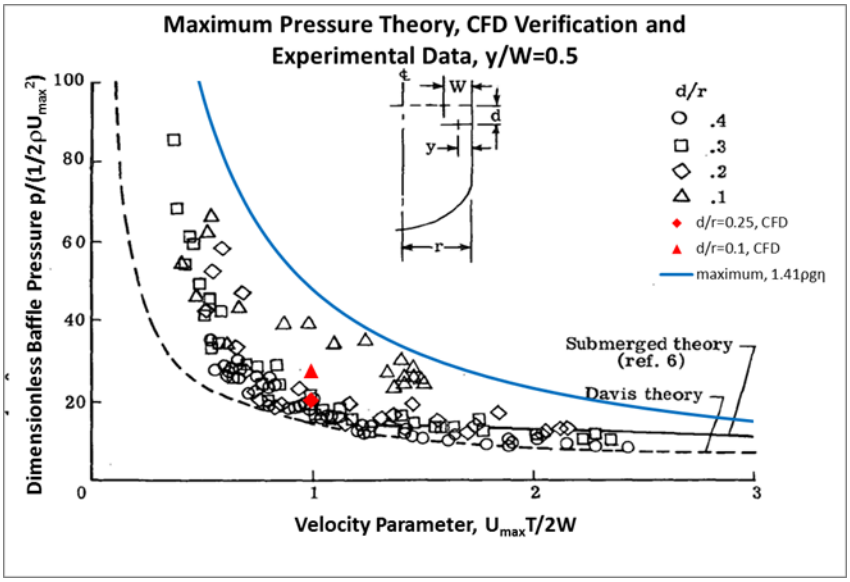

(a) Submerged baffle

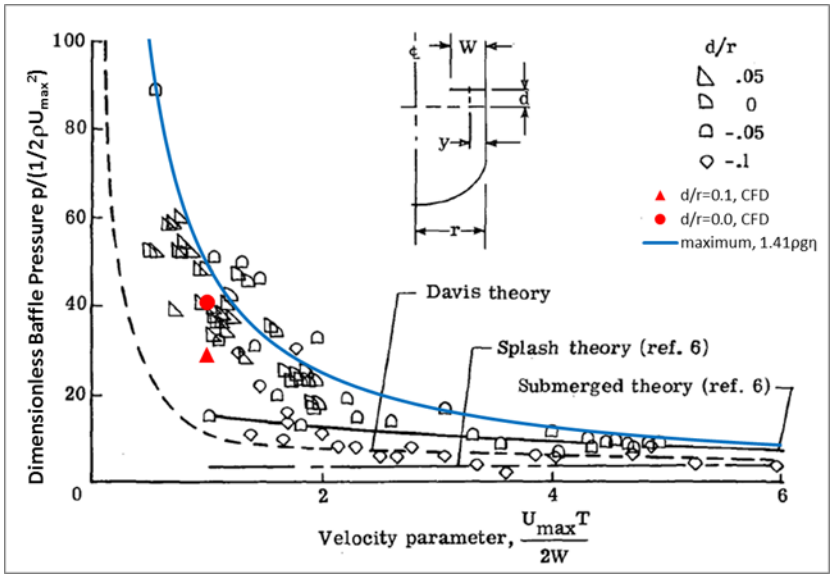

(b) Baffle near the free surface

Figure 8. Pressure comparison at mid of the baffle ($y/W = 0.50$) between experimental data, previous theories, CFD, and the current maximum pressure theory.

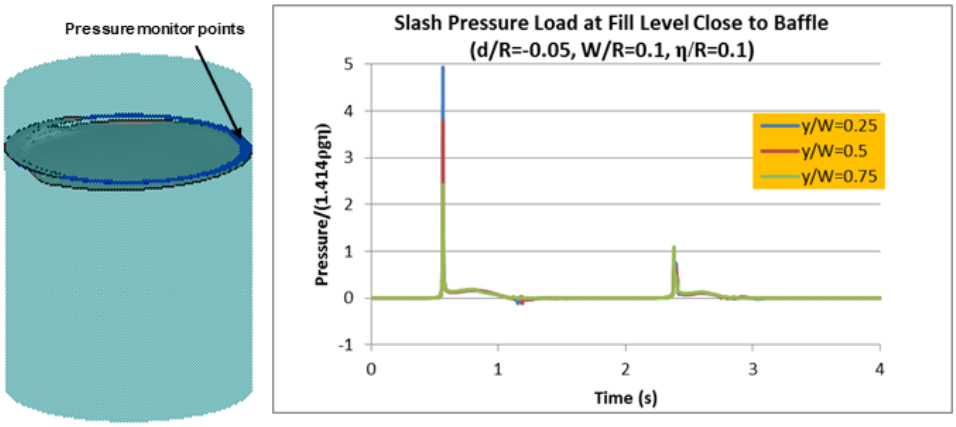

Figure 9. Computed high-pressure spike due to splash during slosh when the baffle is slightly above the free surface.

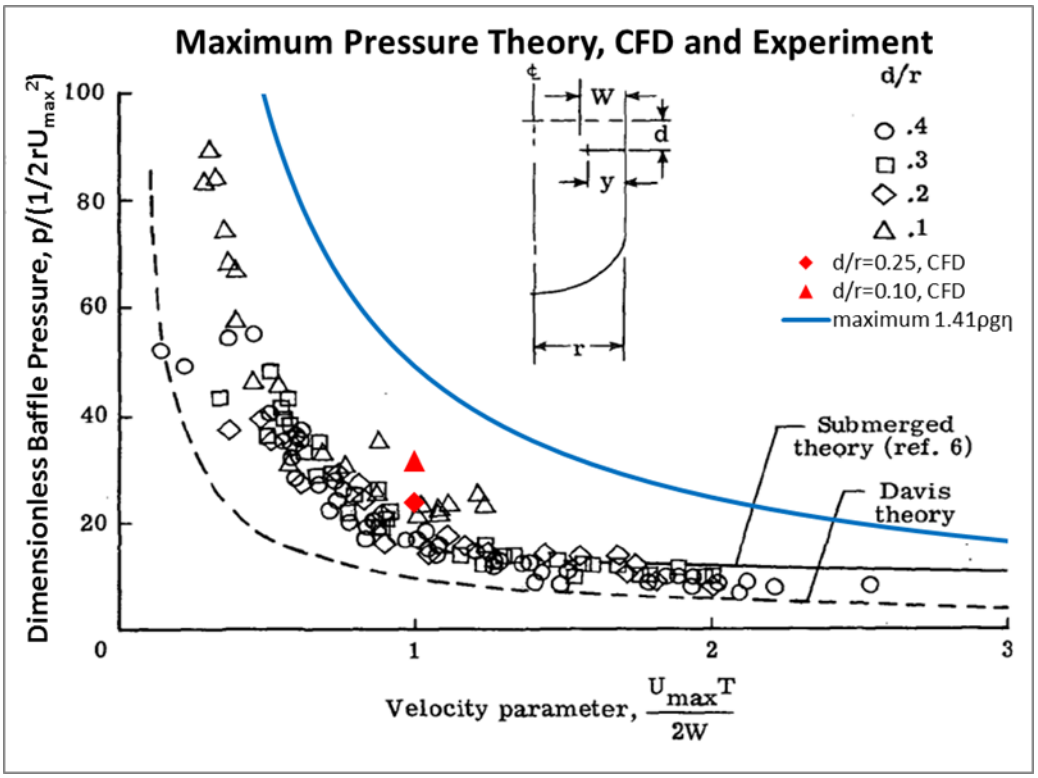

Figure 10. Pressure comparison at the tip of the baffle ($y/W = 0.75$) between experimental data, previous theories, CFD, and the current maximum pressure theory

SUMMARY AND CONCLUSIONS

This study derived a theory for the maximum pressure load on a slosh baffle based on the energy conservation principle. It is verified from CFD that pressure in the slosh flow field can be decomposed into static and transient components. The maximum transient amplitude is $\rho g \eta$, where η is the initial wave height. CFD results verify that there is indeed a phase shift in pressure across the baffle. This shift angle depends on the fluid damping, with higher damping leading to a greater phase shift. The theory predicts that the maximum pressure load occurs when the phase shift angle is 90 degrees.

Comparison with CFD simulations verified the proposed theory: the maximum pressure load occurs when the phase shift is 90 degrees with a value of 1.41ρgη. Comparison to an extensive historical experimental data set validated the theory. When the baffle is submerged, the maximum pressure theory envelopes all the experimental data points, and the theory is a conservative estimate of the baffle load. When the baffle is uncovered, a subset of the data exceeds the theory.

CFD simulation results at fill levels near the baffle location revealed that the theory still envelopes baffle loads applied at the slosh frequency, but localized high-pressure high frequency splash induced loads were also observed. Splash loads and slosh loads should be separated as distinct phenomena for load analyses due to how differently they transfer energy to the baffle structure. Given the observed dynamics when uncovering the baffle, it is believed that the experimental data at fill levels very near the baffle location contains both slosh and splash loads. The pedigree of the data and data analysis is not fully known, so it is impossible to verify if the reported pressures do contain splash loads. However, the presented understanding of slosh dynamics, along with the validation and verification shown, promote confidence in the proposed theory and the need for a separate assessment of splash-induced loads.

The proposed maximum pressure load theory has a simple expression and can be applied to the structural design of slosh baffles.

REFERENCES

1. H. Q. Yang and J. W. Peugeot, Propellant Sloshing Parameter Extraction from CFD Analysis, *Journal of Spacecraft and Rockets*, Vol. 51, No. 3 (2014), pp. 908-916.
2. H. N. Abramson, “The Dynamic Behavior of Liquids in Moving Containers,” NASA SP-106, 1967.
3. J. W. Miles, “On the Sloshing of Liquid in a Cylindrical Tank. Report. No. AM6-5, Gal-TR-18, The Ramo-Wooldridge Corp., Guided Missile Research Div., Apr. 1956.
4. Liu, F.C., “Pressure On Baffle Rings Due To Fuel Sloshing In A Cylindrical Tank,” NASA-MSFC Aero-Astrodynamics Internal Note 4-64, January 1964.
5. Scholl, H.F., Stephens, D.G., Davis, P.K., “Ring-Baffle Pressure Distribution and Slosh Damping In Large Cylindrical Tanks,” NASA TN D-6870 (1972).
6. Braslow, A. L., “Propellant Slosh Loads,” NASA Space Vehicle Design Criteria (Structures), NASA SP-8009, 1968.
7. Keulegan, G.H., Carpenter, L.H., “Forces On Cylinders And Plates In An Oscillating Fluid,” Journal of Research of the National Bureau of Standards (1958).
8. Miles, J.W., “Ring Damping Of Free Surface Oscillations In A Circular Tank,” Journal of Applied Mechanics (1958).